Cite this: *J. Mater. Chem. B*, 2014, **2**, 1539

Tough nanocomposite double network hydrogels reinforced with clay nanorods through covalent bonding and reversible chain adsorption†

Guorong Gao, Gaolai Du, Yajun Cheng and Jun Fu*

Polymer hydrogels with superior strength and toughness are potential candidate materials for the replacement or engineering of load-bearing tissues. This manuscript reports novel tough nanocomposite hydrogels with an unusual energy dissipation mechanism based on both covalent and physical interactions between clay nanorods and polymer chains. Attapulgite (ATP) nanorods grafted with vinyl groups on the surface served as macro-crosslinkers to copolymerize with 2-acrylamido-2-methylpropane-sulfonic acid (AMPS) to form an initial nanocomposite network, which subsequently hosted the polymerization of acrylamide (AAm) monomers to generate a novel nanocomposite double network (DN) hydrogel. The morphology, swelling behavior and compressive properties of the ATP-grafted DN hydrogels were investigated as a function of ATP content (C_{ATP}), in comparison with the ATP-filled DN gels. With a clay content between 0.1 wt% and 1.0 wt%, the nanocomposite hydrogels did not fracture up to a compressive strain of 98%, exhibiting an initial modulus (E) up to 0.36 MPa, a compressive strength higher than 65.7 MPa, and a work to fracture (or fracture energy) higher than 2.6 MJ m^{-3}, in comparison to 0.19 MPa, 18.6 MPa, and 1.1 MJ m^{-3} for the conventional DN gels. Cyclic loading–unloading tests showed abnormal residual energy dissipation even though the rigid PAMPS network had fractured. Such viscous energy dissipation decayed during cyclic loading, and could be restored depending on time and temperature. This is related to the reversible desorption–re-adsorption of polymer chains from the clay surface. Possible reinforcing and fracture mechanisms are discussed.

Introduction

Polymer hydrogels, soft materials consisting of physically or chemically cross-linked polymer networks with high water content,[1] have been widely recognized as candidate materials for the replacement and/or repair of tissues or organs based on the concept of tissue engineering.[2] The mechanical properties of hydrogels, including strength, toughness, and stiffness, are critical to cell growth and tissue regeneration. Strong and tough hydrogels are of special interest for the repair or regeneration of load-bearing bio-tissues, such as cartilages, tendons, and ligaments, that present excellent mechanical properties including high toughness, shock absorbance, low sliding friction (cartilage), and/or robust contraction (muscle).[3,4] Most synthetic and natural hydrogels, however, are weak and fragile.

Enormous efforts have been devoted to developing hydrogels with extraordinary toughness and strength. Double network hydrogels (DN gels)[5] and nanocomposite gels (NC gels)[6] are two types of tough hydrogels. DN gels are comprised of a *contrast structure*,[7] in which the first network is a tightly crosslinked rigid polyelectrolyte, while the second network is a loosely crosslinked flexible neutral polymer interpenetrating the first network. Upon loading, the rigid PAMPS network fractures into fragments that serve as physical and partly chemical cross-linkers for the soft and ductile PAAm to sustain high stress and strain.[8] Due to the irreversible fracture of the first network, the hydrogel loses its capability to dissipate energy upon subsequent loading and behaves like a rubber. The subsequent loading–unloading curves overlap, and the residual energy dissipating loops are negligible.[9,10] This has been a major limitation of DN gels for applications as tissue substitutes.

Tough and resilient nanocomposite hydrogels (NC gels) are usually synthesized by *in situ* polymerization of hydrophilic monomers in the presence of exfoliated clay (*e.g.*, laponite[11–14]) nanosheets as physical crosslinking junctions to strongly adsorb the polymer chains (*e.g.*, poly(*N*-isopropylacrylamide)[15–17] or polydimethylacrylamide[18,19]) on the clay surface. On average, each clay platelet may adsorb several polymer chains, while a single ultra long polymer chain ($\sim 10^6$ g mol^{-1})[20] may adhere onto several clay platelets, resulting in the formation of physical networks. At large strains, the highly stretched polymer

Ningbo Key Laboratory of Polymer Materials, Polymers and Composites Division, Ningbo Institute of Materials Technology & Engineering, Chinese Academy of Sciences, 519 Zhuangshi Road, Zhenhai District, Ningbo 315201, China. E-mail: fujun@nimte.ac.cn; Fax: +86-574-86685176; Tel: +86-574-86685176

segments or chains detach from the clay surface, allowing for a large strain of up to 3500%.[11] Thus, the energy dissipation is a sum of the entropic elasticity of the chains and the enthalpic contribution from the polymer–clay interactions. Upon unloading, the elastic deformation of the polymer chains recovers, and some of the detached chains/segments re-adsorb onto the clay surface.[11,21–25]

Most recently, the combination of nanoparticles and the double network concept has been demonstrated to be effective in generating tough hydrogels.[26,27] Silica nanoparticles strongly adsorb polymer chains and significantly improve the strength and toughness of hydrogels.[28–30] The adsorbed polymer layer on the surface of the silica particles forms core–shell structures that presumably account for the superior toughness.[29] Previously, we have used surface-functionalized silica particles as multi-functional crosslinkers for the synthesis of a PAMPS network of DN gels.[31] As a result, the nanocomposite DN hydrogels sustained a compressive strain of up to 98% and stress above 70 MPa without fracturing.[31] The covalent bonding and physical adsorption of polymer chains onto silica nanoparticles are suggested to account for the high mechanical strength and toughness. Dong *et al.*[32] introduced bare carbon nanotubes into the first network of PAMPS/PAAm DN hydrogels, which improved the strength and toughness.

In this work, novel nanocomposite double network hydrogels were synthesized by using surface-modified attapulgite (ATP) nanorods as macro-crosslinkers to copolymerize with conventional PAMPS/PAAm double network hydrogels (Scheme 1). The ATP nanorods, with a diameter of 20–30 nm and a length of 200–1000 nm, contain exchangeable cations in the framework channels and reactive –OH groups on surface,[33] which allow for the physical adsorption of polymer chains on the surface[34] and convenient surface chemical modification with functional groups.[35] Both surface-grafted and bare ATP nanorods are used to form composites with the DN gels. The morphologies, swelling behavior and compressive properties of these novel nanocomposite DN gels are compared. These nanocomposite hydrogels show extraordinary compressive strength and toughness, depending on the clay content. Moreover, the reversible desorption–re-adsorption of polymer chains, as well as covalent bonding, to the clay surface imparts residual capability to dissipate energy despite the permanent damage of the rigid PAMPS network.

Experiments

Materials

Attapulgite (ATP, Jiuchuan Nano-Material Technology Co. Ltd., Jiangsu, China) was dried in vacuum at 110 °C for 48 h before use. Ethanol (A. R.), vinyltriethoxysilane (VTEOS, C. P.), acetic acid (AAc, A. R.), acrylamide (AAm, A. R.), and potassium persulfate (KPS, A. R.) were purchased from the Sinopharm Chemical Reagent Co., Ltd., and used as received. 2-Acrylamido-2-methylpropane-sulfonic acid (AMPS, 98%, Aladdin Chemistry Co. Ltd.) and *N*,*N*′-methylene-bisacrylamide (MBAA, 99%, Aladdin) were recrystallized from methanol before use. Deionized (DI) water was bubbled with nitrogen gas for more than 1 h prior to use.

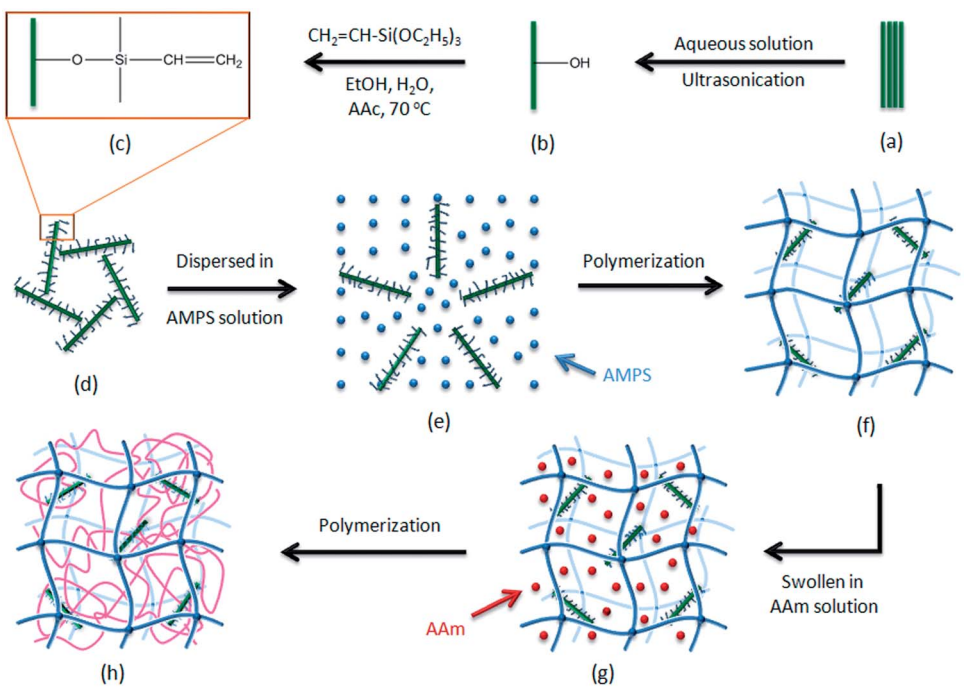

Scheme 1 (a–c) Schematic depiction of the surface modification of exfoliated attapulgite. The modified ATP nanorods (d) were mixed with AMPS monomers (e) for polymerization to yield a nanocomposite PAMPS hydrogel (f), which was swollen in AAm solution (g), followed by polymerization to create a final nanocomposite double network hydrogel (h).

Modification of ATP with VTEOS

ATP (2 g) was sonicated in EtOH–water (75 mL : 75 mL) for 2 h. Then, a solution of VTEOS (5 mL) in water (45 mL) was added under vigorous stirring, followed by acidification to pH 3.0 with AAc. The mixture was then transferred into a flask and refluxed at 70 °C for 30 min. Finally, the suspension was centrifuged and washed with deionized water to pH 7.0, followed by washing with ethanol 3 times. The product, V-ATP, was lyophilized for use.[36]

Preparation of double network hydrogels

Double network hydrogels were synthesized by a two-step sequential free-radical polymerization method as described previously.[31] In the first step, 4 mol% MBAA and 0.1 mol% initiator KPS with respect to AMPS were added to a 1 M AMPS solution. After being bubbled with nitrogen gas for 30 min, the solution was transferred into a mold consisting of two glass plates separated by a 2 mm silicone rubber spacer. The mold was placed in a water bath at 60 °C for 10 h for the polymerization and gelation of AMPS. In the second step, the PAMPS gel was swollen in a large amount of aqueous solution containing 3 M AAm, 0.01 mol% MBAA and 0.01 mol% KPS for 1 day until equilibrium was reached. The swollen PAMPS gel was sandwiched by two glass plates and heated at 60 °C for 10 h in a water bath to polymerize the AAm. Finally, the gels were swollen in a large excess of water for 1 week, with the water being changed every day to remove the residual chemicals.[37,38]

Preparation of nanocomposite DN gels

The synthesis procedure of nanocomposite DN gels is the same as described above, except that in the first step an aqueous dispersion of V-ATP (0.1, 0.5, 1, 1.5 and 2 wt% with respect to AMPS) was added into the aqueous AMPS solution with sonication, followed by the routine synthesis procedure of DN gels (Scheme 1). For comparison, bare ATP was also blended with the AMPS solution for the synthesis of DN gels. The resulting gels were named as DN*m*A-V for the ATP-grafted nanocomposite DN, and DN*m*A for the ATP-filled DN gels, with DN indicating the double network hydrogels, A indicating attapulgite, V indicating VTEOS, and *m* indicating the weight ratio (wt%) of ATP to AMPS.

Fourier transform infrared spectroscopy (FTIR)

ATP/KBr and V-ATP/KBr platelets were scanned using a Nicolet 6700 spectrometer (Thermo Fisher Scientific, United States) in the range of 400–4000 cm^{-1} at a resolution of 4 cm^{-1} with an average of 32 scans.

Transmission electron microscopy (TEM)

The suspensions of attapulgites or modified ATP were cast on carbon-coated copper grids and dried at room temperature for TEM imaging. The nanocomposite DN gels were embedded in epoxy resin for cryo-microtoming at −40 °C with a glass knife to *ca.* 50 nm thick sections using a PT-XL ultra-microtome (RMC Corporation). The thin sections were collected onto copper grids for imaging using a transmission electron microscope (Tecnai F20, FEI Inc., Oregon) with an accelerating voltage of 200 kV.

Scanning electron microscopy (SEM)

For SEM imaging, the hydrogels were freeze-fractured in liquid nitrogen and freeze-dried. The fracture surfaces of the dehydrated gels were sputtered with a thin layer of platinum for SEM scanning using a Hitachi S4800 instrument (Hitachi, Japan) at an accelerating voltage of 15 kV.

Swelling behavior of hydrogels

To determine the equilibrium swelling ratio (ESR) of the gels, a small fully swollen hydrogel sample with an original weight W_0 was successively dried at 80 °C for 12 h and at 25 °C in a vacuum oven for 48 h to approach a dry weight W_d. The ESR was calculated using the equation $ESR = (W_0 - W_d)/W_d \times 100\%$. Eight samples were tested for each gel to obtain the average ESR.

Compression and cyclic compression tests

The mechanical properties of the hydrogels were measured with an Instron 5567 (Instron Inc, MA) instrument in compression mode. Five specimens were tested for each hydrogel. Each specimen was coated with a thin layer of silicon oil to prevent water evaporation.

For the compression tests, a cylindrical sample (9 mm diameter and 5–7 mm height) was compressed at a strain rate of 10% min^{-1} with a 10 kN load cell. The maximum compression limit was set at 98% strain to protect the load cell. The nominal stress, σ, was calculated approximately using $\sigma = F/\pi R^2$, where F is the load force and R is the original radius of the specimen. The nominal strain (ε) under compression was defined as the change in height (h) relative to the original height (h_0) of the freestanding specimen, $\varepsilon = (h_0 - h)/h_0 \times 100\%$. The initial modulus ($E$) was calculated as the slope of the compressive stress–strain curve within the range ε = 5–10%. The fracture toughness of hydrogels was characterized by the fracture energy density, or work to fracture (U, MJ m^{-3}), which was obtained by integrating the area under the stress–strain curve:[39]

$$U = \int \sigma d\varepsilon$$

Cyclic compressive loading–unloading tests were performed immediately after the first loading–unloading cycle on fresh samples. After cyclic tests, the samples were kept in silicone oil at different temperatures for different durations. Then compression tests were conducted on these samples for comparison with the previous cyclic compression data.[40]

Results and discussion

Morphology and structure of double network hydrogels with modified ATP nanorods

The surface modification of attapulgite with VTEOS was verified by the new Si–O–Si bands appearing in the FTIR spectrum at 1120, 1080, 1031, and 790 cm^{-1},[41–44] as well as those at 3062 cm^{-1} (=CH_2 asymmetric stretch), 1600 cm^{-1} (C=C stretch) and 1274 cm^{-1} (=CH in-plane bend) (Fig. 1c).[45] The modified nanorods appear hairy under TEM observation (Fig. S1a†), in contrast to

the smooth surface of bare ATP (Fig. S1b†). The diameter and length of the ATP nanorods were not affected by the surface modification.

The nanocomposite hydrogels show typical porous structures (Fig. 2a–f). The ATP nanorods are well dispersed in the polymer matrix (Fig. 2g). The content of ATP nanorods has a remarkable influence on the pore size of the hydrogels: as the ATP content (C_{ATP}) increases from 0.1 to 1 and 2 wt%, the pore size decreased rapidly (Fig. 2h). For each C_{ATP}, the DN*m*A gels (Fig. 2d–f) showed larger average pore size than those of the DN*m*A-V gels (Fig. 2a–c), although the differences are not statistically significant (Fig. 2h). The dense porous structures with high ATP content may indicate a densely crosslinked structure. In addition to the physical adsorption of polymer chains onto the ATP nanorods, the covalent bonding of polymer chains on the vinyl-functionalized surface may result in a higher crosslink density in the DN*m*A-V gels than in the DN*m*A gels.

The hydrogels show lower equilibrium swelling ratios (ESR) with increasing ATP content (Fig. 3). In the DN hydrogels, the swelling is predominantly determined by the balance of the elasticity of the first network and the osmotic pressure of the second neutral network, owing to their contrasting structures.[46] Here, the decrease in swelling ratio is mainly attributed to the higher elasticity of the dense porous network with increasing C_{ATP} (Fig. 2) through covalent bonding or physical adsorption of polymer chains onto the ATP surface. At each C_{ATP}, the ESR value is lower for the DN*m*A-V gels than for the DN*m*A gels. These observations further indicate the denser network of the nanocomposite DN gels than the clay-free DN gel.

Mechanical properties of the DN*m*A-V and DN*m*A hydrogels

The compressive properties, including elastic modulus (E), stress at 90% strain ($\sigma_{c,0.9}$), fracture stress ($\sigma_{c,f}$), fracture strain ($\varepsilon_{c,f}$), and fracture toughness (U), of the nanocomposite DN hydrogels are summarized in Table 1. The hydrogels did not fracture up to 98% strain with $C_{ATP} \leq 1.0$ wt%. For DN*m*A-V, fracture strength and fracture toughness were improved to above 65.7 MPa and 2.6 MJ m^{-3} at a C_{ATP} of 1.0 wt%, in comparison to 18.6 MPa and 1.1 MJ m^{-3} for the conventional DN gel. Further increases in C_{ATP} led to decreases in the fracture stress and strain and the fracture toughness, which might be attributed to the increased rigidity of the network having more crosslinks and entanglements with the higher clay content. However, these values are still higher than those of the nanorod-free double network hydrogels. At each C_{ATP} value, DN*m*A-V showed a higher modulus, compressive stress, and fracture toughness than for the corresponding DN*m*A. At $C_{ATP} >$ 1.0 wt%, the fracture properties of DN*m*A-V decreased slightly, while those for the DN*m*A decayed more rapidly with the increasing ATP nanorod content. Strong physical adsorption and/or covalent bonding between polymer chains and nanorods have been recognized to improve the strength and stiffness of nanocomposite hydrogels.[16] The strong physical adsorption of PAAm chains with the ATP nanorods was verified by the *in situ* polymerization of AAm monomers in the presence of bare ATP nanorods in an aqueous solution, which resulted in a hydrogel without using any crosslinking agents. In contrast, the AMPS solution did not gel during *in situ* polymerization with ATP (Fig. S2†). These results indicate the strong physical adsorption between the PAAm chains and the clay nanorods. Similar strong physical adsorption of polymer chains to clay surfaces has been thought to account for the super toughness of polymer–clay nanocomposite hydrogels due to energy dissipation through the desorption of polymer chains from the clay surface.[13]

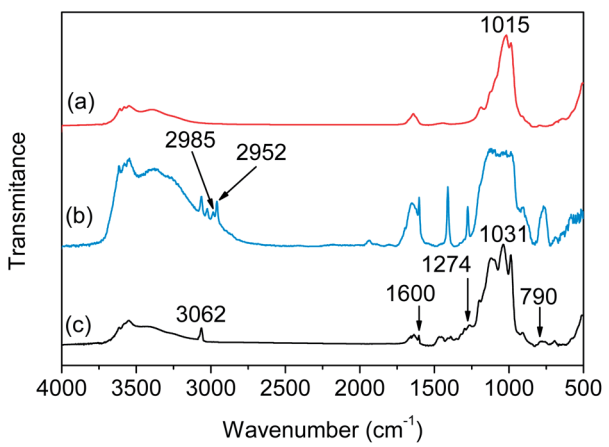

Fig. 1 FTIR spectra of (a) attapulgite (ATP), (b) a mixture of vinyltriethoxysilane (VTEOS) and ATP, (c) and the VTEOS-modified ATP nanorods.

Hysteresis: energy dissipation of the nanocomposite double network hydrogels

In the nanocomposite double network hydrogels, the strong polymer–clay adsorption enables residual energy dissipation after the rupture of the PAMPS network. This property was demonstrated by performing second loading–unloading tests at $\varepsilon = 0.90$ following the first test to the same strain on fresh hydrogels. The second loading–unloading curves showed obvious hysteresis loops for the DN*m*A-V (Fig. 4b) and DN*m*A (Fig. 4c) hydrogels, in comparison to the overlapped loading–unloading curves of the clay-free DN gel after the rupture of the rigid AMPS network (Fig. 4a).[8]

The energy dissipation by the hydrogels, ΔU, is defined as the area of the hysteresis loop encompassed by the loading–unloading curve:[47]

$$\Delta U = \int_{\text{loading}} \sigma_{\text{comp}} d\varepsilon - \int_{\text{unloading}} \sigma_{\text{comp}} d\varepsilon$$

The energy dissipation of the first loading–unloading cycle (ΔU^{1st}) increased linearly with the C_{ATP} value (Fig. 4d). This result is in accordance with the SEM images in Fig. 2, and the swelling behavior in Fig. 3. The dense porous structures may stem from the strong adsorption of polymer chains onto the surface of ATP. The ΔU^{1st} values of the DN*m*A-V gels were higher than those of the DN*m*A gels, with the difference increasing with C_{ATP} (Fig. 4d).

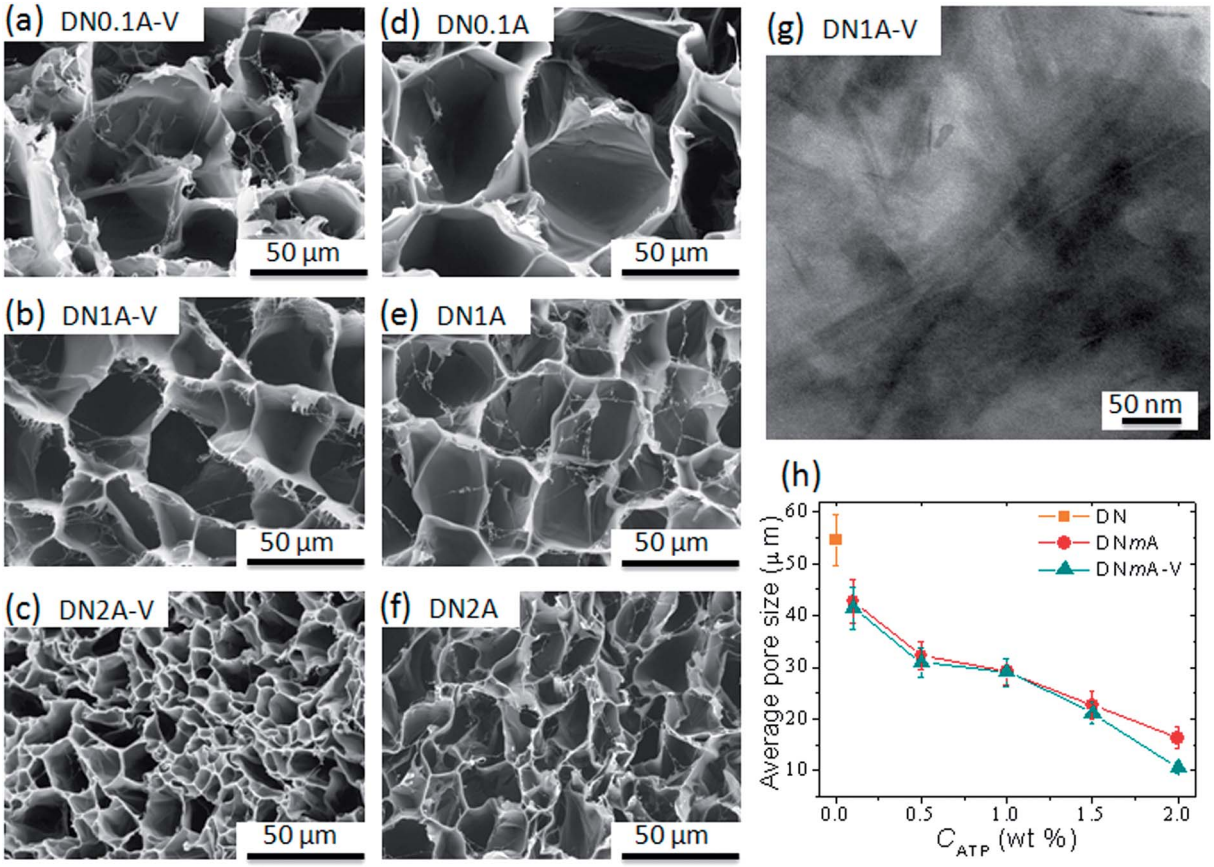

Fig. 2 SEM images of (a–c) DN*m*A-V, and (d–f) DN*m*A after lyophilization, with ATP contents of (a and d) 0.1, (b and e) 1.0, and (c and f) 2.0 wt%. (g) TEM image of DN1A-V. (h) The average pore size of DN*m*A and DN*m*A-V as a function of clay content.

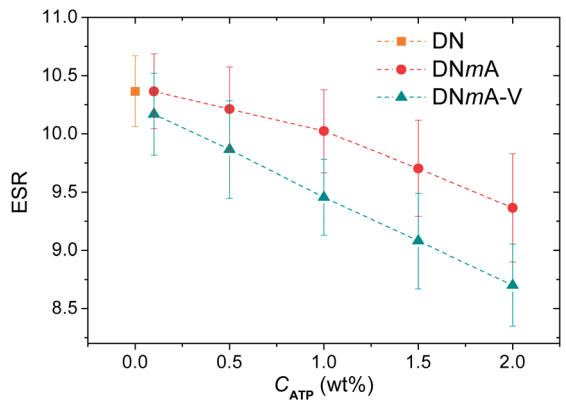

Fig. 3 The effect of clay content (C_{ATP}) on the equilibrium swelling ratio (ESR) of the nanocomposite double network hydrogels. The dashed lines are guides for the eye.

The ΔU^{2nd} values of the second loading–unloading tests reflect the energy dissipation other than that caused by the rupture of the rigid PAMPS network. The ΔU^{2nd} values for the DN*m*A and DN*m*A-V increased with C_{ATP} (Fig. 4e), with the values of the latter being higher than those of the former. Under high strain, desorption of polymer chains from the clay surface dissipates energy. Moreover, for the DN*m*A-V, the combined contributions from both the physical adsorption and covalent bonding may account for the higher energy dissipation during the second loading–unloading tests.

The contribution from the polymer–clay interaction to the overall energy dissipation can be evaluated by dividing ΔU^{2nd} by ΔU^{1st} (Fig. 4f). With the increasing clay content, the ratio $\Delta U^{2nd}/\Delta U^{1st}$ increases, indicating an increasing contribution from the polymer–clay interaction to the energy dissipation mechanism of the nanocomposite hydrogels. The ratio for DN*m*A-V is higher than that for DN*m*A, indicating the increased contribution of polymer chain detachment from the nanorods in the DN*m*A-V. A possible interpretation of this is as follows: when ATP is covalently fixed in the first network, the PAAm chains penetrate through the covalent networks reversibly adsorbed onto the clay surfaces, and may adopt conformations such as trains, loops and entanglements with covalent bonds on the ATP surface. The PAAm chains are restricted by neighboring covalent bonds and are difficult to peel off from clay surface compared to in the ATP-filled hydrogels.

The energy dissipation from desorption (ΔU^{2nd}) is only 12% (DN2A-V) of that of the rupture energy of the DN gel, due to the permanent damage of the sacrificial PAMPS network. However, it is interesting that such a small energy dissipation was recoverable, primarily due to the reversible desorption–re-adsorption of polymer chains onto the clay surface. This will be discussed below.

Table 1 The compressive properties of nanocomposite double network hydrogels (mean ± standard deviation)

Gel	C_{ATP} (wt%)	E (MPa)	$\sigma_{c,0.9}$ (MPa)	$\sigma_{c,f}$[a] (MPa)	$\varepsilon_{c,f}$ (%)	U[a] (MJ m^{-3})
DN	0	0.19 ± 0.01	4.9 ± 0.3	18.6 ± 1.8	95 ± 0.6	1.1 ± 0.1
DN*m*A-V	0.1	0.25 ± 0.02	5.1 ± 0.4	>47.1 ± 2.9	>98%[b]	>1.9 ± 0.12
	0.5	0.29 ± 0.02	5.8 ± 0.5	>55.8 ± 5.5	>98%[b]	>2.2 ± 0.14
	1	0.36 ± 0.03	6.2 ± 0.3	>65.7 ± 3.1	>98%[b]	>2.6 ± 0.09
	1.5	0.42 ± 0.04	6.9 ± 0.4	61.5 ± 7.2	97.2 ± 0.4	2.6 ± 0.15
	2	0.53 ± 0.05	10.6 ± 1.2	42.3 ± 2.9	96.5 ± 0.2	2.5 ± 0.06
DN*m*A	0.1	0.24 ± 0.02	5.0 ± 0.5	>43.5 ± 3.3	>98%[b]	>1.9 ± 0.14
	0.5	0.26 ± 0.02	5.1 ± 0.2	>55.3 ± 3.8	>98%[b]	>2.2 ± 0.08
	1	0.30 ± 0.03	5.5 ± 0.5	>58.7 ± 4.0	>98%[b]	>2.3 ± 0.12
	1.5	0.38 ± 0.03	5.8 ± 0.2	35.8 ± 3.2	95.8 ± 0.1	1.9 ± 0.18
	2	0.43 ± 0.04	7.7 ± 0.3	25.2 ± 2.4	95.1 ± 0.5	1.7 ± 0.1

[a] For gels that do not fracture at 98% strain, the listed stress values are calculated at 98% strain. [b] These hydrogels do not fracture at strain of 98%.

Energy dissipation upon cyclic loading–unloading tests

The contribution from the covalent bonding and physical adsorption to the energy dissipation was further investigated by cyclic compressive loading–unloading tests of the DN*m*A and DN*m*A-V gels. The cyclic loading–unloading tests with 90% strain led to a slight drop of the loading curve, while the $\sigma_{c,0.90}$ value remains constant (Fig. 5a). As a result, the area of the hysteresis loop decayed in the second, third, fourth, and fifth cycles, eventually reaching a plateau value (Fig. 5b). These values are higher than those of the conventional DN gels. Again, the ΔU values of DN*m*A-V were higher than those of the DN*m*A, but the difference between them diminished with further testing (Fig. 5b). The decay of energy dissipation capability of these nanocomposite hydrogels indicates a viscous dissipation mechanism primarily based on the gradual desorption of the polymer chains from the clay nanorods. In contrast, the DN hydrogels maintained a low dissipation of around 10 kJ m^{-3} during the cyclic tests, which may originate from the very small amount of chemical bonding between the PAMPS and PAAm chains.[38]

Reversible desorption–re-adsorption of polymer chains onto the clay surface

The decayed viscous dissipation could be restored by the re-adsorption of the polymer chains onto the clay surface. This was

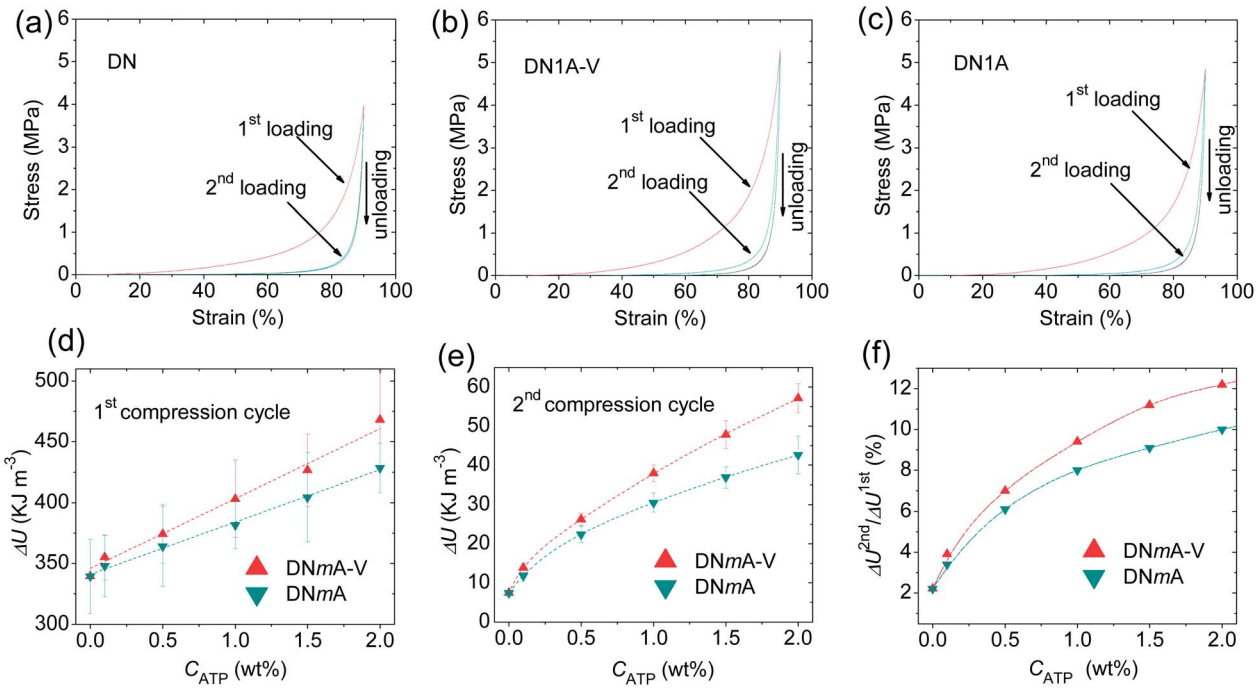

Fig. 4 Representative compression loading and unloading curves of (a) DN, (b) DN1A-V, and (c) DN1A. The energy dissipation of the consecutive (d) first and (e) second compression cycles of DN*m*A-V and DN*m*A as a function of clay content. (f) The energy dissipation ratio of the second loading–unloading loop (ΔU^{2nd}) to that of the first cycle (ΔU^{1st}) for the nanocomposite DN gels as a function of the clay content. The dashed lines are a guide to the eye.

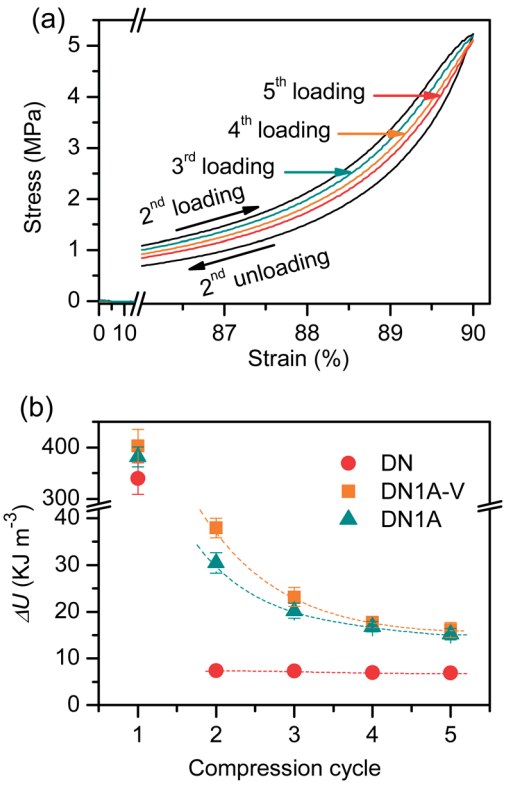

Fig. 5 (a) Representative cyclic loading–unloading curves of DN1A-V for five sequential test cycles without waiting. (b) The decay of energy dissipation for DN1A-V and DN1A with increasing cycle numbers.

realized by restoring the tested samples at different temperatures for certain time intervals after the cyclic tests at $\varepsilon = 0.90$. The extent and rate of recovery depended on temperature and time. For example, after storing the 5-cycle-tested hydrogels ($\varepsilon = 0.90$) at 25 or 50 °C, a recovery of the energy dissipation towards the ΔU^{2nd} values (those obtained right after the rupture of the PAMPS network, solid lines in Fig. 6) was achieved when the samples were subjected to compressive loading–unloading tests (*i.e.*, the sixth test).

At 25 °C, it is very difficult for either the DN*m*A-V or DN*m*A gels to reach the original ΔU^{2nd} values for C_{ATP} from 0.1, 1.0, to 2.0 wt% in 12 h. The recovery was accelerated at 50 °C. The ATP-filled hydrogels after 12 h recovery showed ΔU^{6h} values very close to or even slightly higher than their ΔU^{2nd} values, indicating a full recovery of the polymer–clay adsorption. In contrast, the ATP-grafted hydrogels barely achieved a 100% recovery at 50 °C after 12 h.

The extent of recovery is evaluated by a ratio of the sixth energy dissipation to that of the second test, *i.e.*, $\Delta U^{6th}/\Delta U^{2nd} \times 100\%$. The DN*m*A-V gels always showed a lower recovery ratio than the DN*m*A gels (Fig. 6d). During the cyclic tests, the covalent bonding between the polymer chains and the clay nanorods may be permanently damaged, which gradually diminishes the difference between the DN*m*A-V and DN*m*A gels (Fig. 5b). The damage to the covalent bonds is not reversible, leaving a gap between these two kinds of nanocomposite hydrogels on the recovery curve (Fig. 6d).

Recently, Marcellan *et al.*[48] revealed that transient physical interactions between silica nanoparticles and polymer chains allowed for reversible adsorption–desorption. Thus, the "sacrificial" silica/polymer interactions ruptured to release stress and avoided permanent damage to the covalent bonds. Reversible dissipation and recovery were demonstrated on the time scale of 1–10 s.

In our case, the physical adsorption of PAAm chains onto the clay nanorod surface may be reversible, allowing for desorption under high strain to dissipate energy. Beyond the physical adsorption, the covalent bonding between PAMPS and clay nanorods in DN*m*A-V leads to additional stress transfer between the ruptured PAMPS fragments and the PAAm matrix, which may explain the higher energy dissipation than for the DN*m*A.

The recovery rate in these nanocomposite hydrogels may be slower than the time scale of Marcellan's silica/polymer hydrogel at room temperature, probably due to the complex semi-interpenetrating structures of the DN matrix where the ruptured PAMPS fragments are highly entangled with the PAAm. As a result, the ΔU value decays after multiple loading–unloading cycles. Recovery towards the second loading level can be accelerated at elevated temperatures to favor the re-adsorption of PAAm chains onto the clay nanorods. Such recovery behavior has not been addressed in previous work on nanocomposite double network hydrogels reinforced by silica nanoparticles[31] or carbon nanotubes.[32] This is the first demonstration of the combined effects of physical adsorption and covalent bonding of polymer chains onto ATP nanorods on the enhanced energy dissipation of the nanocomposite DN gels. The additional viscous dissipation originated from desorption–re-adsorption between molecular chains and ATP nanorods,[49] and, although relatively small, it may illuminate new studies to develop novel tough and recoverable hydrogels.

Possible fracture mechanism

It is well-known that the rupture of materials is a process of crack growth and propagation leading to the loss of stability.[49,50] First, a defect is produced in the stress concentration area, it propagates gradually to form a macroscopic flaw, and then the crack tip passes through the inner part under further loading. The rigid PAMPS network fractured into clusters, which behave as flexible physical (and slightly chemical) crosslinkers[38] of the PAAm chains.

In the nanocomposite DN hydrogels, the nanorods, either bare or modified, act as multifunctional macro-crosslinkers for the polymer chains on each nanorod. It is likely that the crosslink density near the nanoparticle surface is greater than in the rest of the composite.[51,52] Additionally, some of the PAAm chains adsorbed on the ATP nanorods may act as "anchors".[53] In the case of PAAm on laponite platelets, the adsorbed polymer layers have a thickness of *ca.*10 Å.[24,54] Such polymer chains stored in a compact state contribute to the residual energy dissipation capability. In the DN*m*A-V, both covalent bonding and physical adsorption of PAAm onto the ATP nanorods may dissipate more energy as the crack tip propagates and grows.

Similar to the conventional DN hydrogels, the fracture of the rigid PAMPS network is irreversible. The hysteresis of the

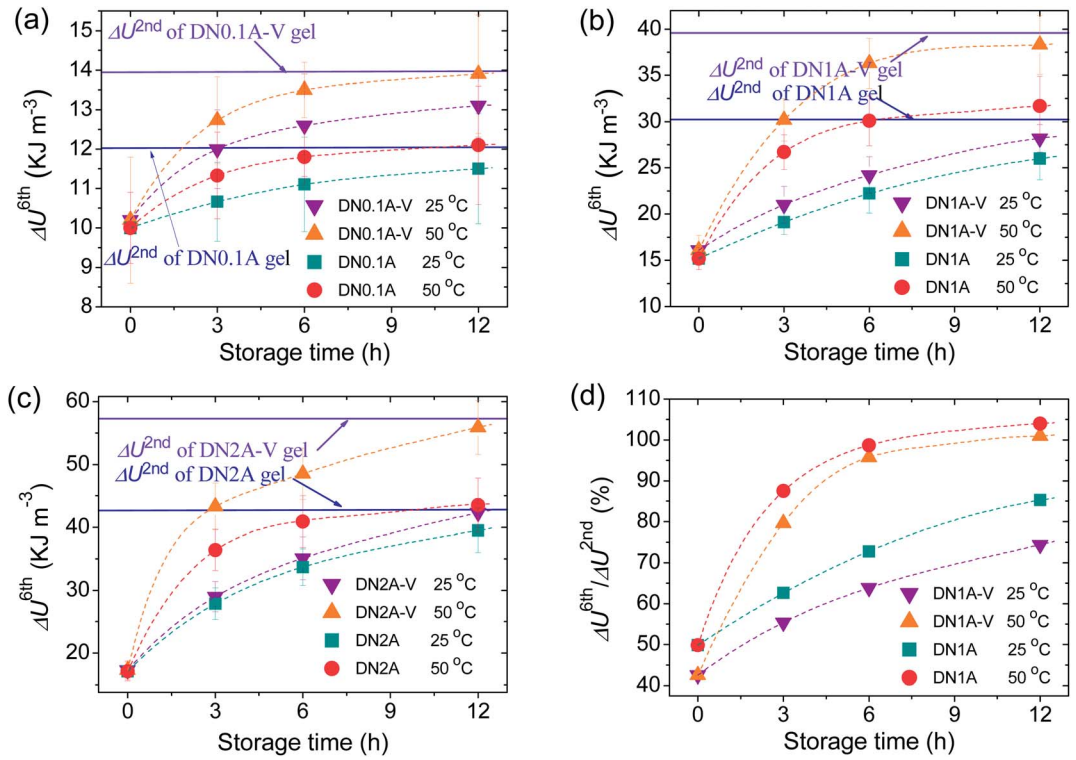

Fig. 6 The energy dissipation of DN*m*A and DN*m*A-V in the sixth compressive loading–unloading test (ΔU^{6th}) after recovery at 25 and 50 °C for up to 12 h following five cyclic loading–unloading tests. The values are compared with those of the second loading–unloading test, the test carried out immediately after the rupture of the rigid PAMPS network. The clay contents are (a) 0.1, (b), 1.0, and (c) 2.0 wt%. (d) The recovery ratio of DN1A and DN1A-V after restoration at 25 and 50 °C for up to 12 h.

nanocomposite DN gels comes from from the physical adsorption of PAAm chains onto the clay surface (Scheme 2). During the first loading, most energy is consumed in the rupture of the PAMPS network (Scheme 2b and e), and a fraction of the energy is consumed by PAAm chain desorption from the ATP nanorod surface. These detached PAAm chains could gradually re-adsorb onto the surface of the ATP nanorods (Scheme 2c and f), which will dissipate energy upon subsequent loading. That is, the energy dissipation capability is recovered. The adsorption of polymer chains onto the clay nanorod surface can be

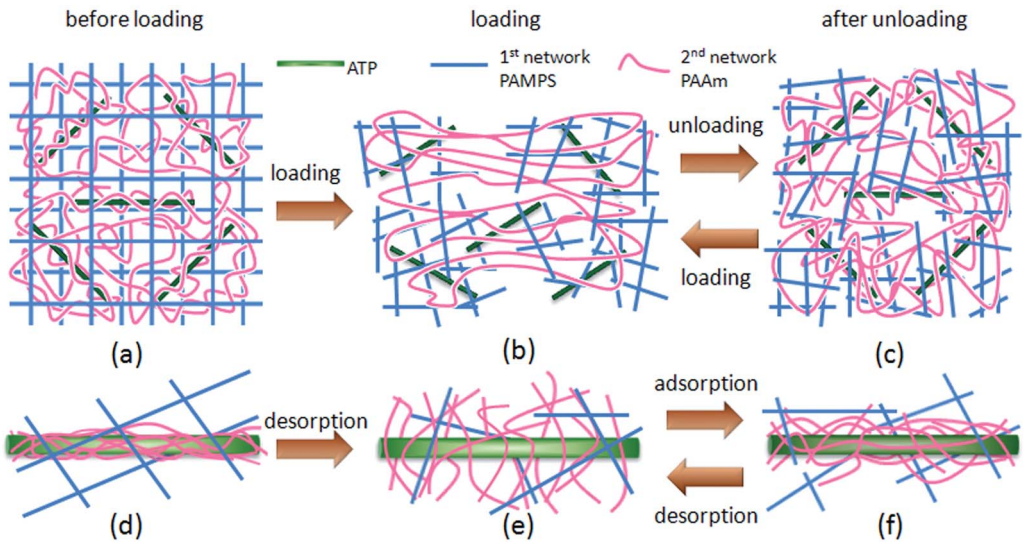

Scheme 2 Schematic illustration of the desorption–adsorption mechanism of the ATP-filled nanocomposite DN gels. (a–c) The possible internal fracture during compressive loading–unloading cycles. (d and e) The desorption of PAAm chains from the ATP nanorods under high stress and strain, and (f) the re-adsorption of polymer chains onto the clay nanorod surface during restoration.

accelerated by increasing the temperature, which has been demonstrated in this study. This finding indicates the possibility of fabricating tough hydrogels that can endure cyclic loading–unloading without completely losing their toughness by introducing strong noncovalent interactions into the DN gels.

Conclusions

ATP nanorods, at low content, have been used to reinforce PAMPS/PAAm double network hydrogels. In the presence of bare ATP nanorods, the modulus, strength, and toughness of DN gels are significantly improved in comparison to those of the conventional DN gels. Moreover, ATP grafted with vinyl groups on the surface, when copolymerized with the DN gels, further improved the strength and toughness of gels. Such nanocomposite DN gels can withstand a compressive strain of up to 98%, stress close to 70 MPa without fracturing, and have a work to fracture higher than 2.6 MJ m^{-3}. Cyclic loading–unloading tests demonstrate hysteresis loops after the fracture of the rigid PAMPS network. The physical adsorption of PAAm chains onto the ATP surfaces may serve as reversible sacrificial bonds and lead to increased energy dissipation efficiency when a load is applied. The damage upon loading partially recovers upon unloading. Such super tough and partially recoverable hydrogels may find applications in biomedical fields, such as in substitutes for load-bearing cartilage, although their biocompatibility remains unknown at this moment.

Acknowledgements

This work was funded by the Natural Science Foundation of China (21004074, 51103172, 212101064), the Hundred Talents Program of the Chinese Academy of Sciences (J. F.), the Zhejiang Natural Science Foundation of China (LR2013B040001), Zhejiang Nonprofit Technology Applied Research Program (no. 2013C33190), the Program for Ningbo Innovative Research Team (2012B82019), and the Scientific Research Foundation for the Returned Overseas Chinese Scholars, State Education Ministry.

Notes and references

1 T. Miyata, *Polym. J.*, 2010, **42**, 277–289.
2 R. E. Webber, C. Creton, H. R. Brown and J. P. Gong, *Macromolecules*, 2007, **40**, 2919–2927.
3 K. Y. Lee and D. J. Mooney, *Chem. Rev.*, 2001, **101**, 1869–1879.
4 M. A. Haque, T. Kurokawa and J. P. Gong, *Polymer*, 2012, **53**, 1805–1822.
5 J. P. Gong, Y. Katsuyama, T. Kurokawa and Y. Osada, *Adv. Mater.*, 2003, **15**, 1155–1158.
6 K. Haraguchi and T. Takehisa, *Adv. Mater.*, 2002, **14**, 1120–1124.
7 T. Nakajima, T. Kurokawa, S. Ahmed, W.-l. Wu and J. P. Gong, *Soft Matter*, 2013, **9**, 1955–1966.
8 J. P. Gong, *Soft Matter*, 2010, **6**, 2583–2590.
9 J. Hu, T. Kurokawa, T. Nakajima, T. L. Sun, T. Suekama, Z. L. Wu, S. M. Liang and J. P. Gong, *Macromolecules*, 2012, **45**, 9445–9451.
10 Y. H. Na, Y. Tanaka, Y. Kawauchi, H. Furukawa, T. Sumiyoshi, J. P. Gong and Y. Osada, *Macromolecules*, 2006, **39**, 4641–4645.
11 K. Haraguchi and H. J. Li, *Macromolecules*, 2006, **39**, 1898–1905.
12 Y. Liu, M. Zhu, X. Liu, W. Zhang, B. Sun, Y. Chen and H.-J. P. Adler, *Polymer*, 2006, **47**, 1–5.
13 O. Okay and W. Oppermann, *Macromolecules*, 2007, **40**, 3378–3387.
14 L. Xiong, X. Hu, X. Liu and Z. Tong, *Polymer*, 2008, **49**, 5064–5071.
15 K. Haraguchi and H. J. Li, *Angew. Chem., Int. Ed.*, 2005, **44**, 6500–6504.
16 J. Wang, L. Lin, Q. Cheng and L. Jiang, *Angew. Chem., Int. Ed.*, 2012, **51**, 4676–4680.
17 T. Wang, D. Liu, C. Lian, S. Zheng, X. Liu and Z. Tong, *Soft Matter*, 2012, **8**, 774–783.
18 K. Haraguchi, *Curr. Opin. Solid State Mater. Sci.*, 2007, **11**, 47–54.
19 K. Haraguchi, R. Farnworth, A. Ohbayashi and T. Takehisa, *Macromolecules*, 2003, **36**, 5732–5741.
20 K. Haraguchi, Y. Xu and G. Li, *Macromol. Rapid Commun.*, 2010, **31**, 718–723.
21 A. K. Gaharwar, C. P. Rivera, C.-J. Wu and G. Schmidt, *Acta Biomater.*, 2011, **7**, 4139–4148.
22 K. Haraguchi, T. Takehisa and S. Fan, *Macromolecules*, 2002, **35**, 10162–10171.
23 C. Lian, Z. Lin, T. Wang, W. Sun, X. Liu and Z. Tong, *Macromolecules*, 2012, **45**, 7220–7227.
24 S. Miyazaki, H. Endo, T. Karino, K. Haraguchi and M. Shibayama, *Macromolecules*, 2007, **40**, 4287–4295.
25 S. Miyazaki, T. Karino, H. Endo, K. Haraguchi and M. Shibayama, *Macromolecules*, 2006, **39**, 8112–8120.
26 H. P. Cong, P. Wang and S. H. Yu, *Small*, 2013, DOI: 10.1002/smll.201301591.
27 M. Kato, N. Shoda, T. Yamamoto, R. Shiratori and T. Toyo, *Analyst*, 2009, **134**, 577–581.
28 W.-C. Lin, W. Fan, A. Marcellan, D. Hourdet and C. Creton, *Macromolecules*, 2010, **43**, 2554–2563.
29 J. Yang, L.-H. Deng, C.-R. Han, J.-F. Duan, M.-G. Ma, X.-M. Zhang, F. Xu and R.-C. Sun, *Soft Matter*, 2013, **9**, 1220–1230.
30 J. Yang, C.-R. Han, J.-F. Duan, M.-G. Ma, X.-M. Zhang, F. Xu, R.-C. Sun and X.-M. Xie, *J. Mater. Chem.*, 2012, **22**, 22467–22480.
31 Q. Wang, R. X. Hou, Y. J. Cheng and J. Fu, *Soft Matter*, 2012, **8**, 6048–6056.
32 W. Dong, C. Huang, Y. Wang, Y. Sun, P. Ma and M. Chen, *Int. J. Mol. Sci.*, 2013, **14**, 22380–22394.
33 W. B. Wang and A. Q. Wang, *Carbohydr. Polym.*, 2010, **82**, 83–91.
34 P. Schexnailder and G. Schmidt, *Colloid Polym. Sci.*, 2009, **287**, 1–11.

35 H. B. Lu, H. B. Shen, Z. L. Song, K. S. Shing, W. Tao and S. Nutt, *Macromol. Rapid Commun.*, 2005, **26**, 1445–1450.
36 L. H. Wang and J. Sheng, *Polymer*, 2005, **46**, 6243–6249.
37 H. Tsukeshiba, M. Huang, Y. H. Na, T. Kurokawa, R. Kuwabara, Y. Tanaka, H. Furukawa, Y. Osada and J. P. Gong, *J. Phys. Chem. B*, 2005, **109**, 16304–16309.
38 T. Nakajima, H. Furukawa, Y. Tanaka, T. Kurokawa, Y. Osada and J. P. Gong, *Macromolecules*, 2009, **42**, 2184–2189.
39 K. J. Henderson, T. C. Zhou, K. J. Otim and K. R. Shull, *Macromolecules*, 2010, **43**, 6193–6201.
40 J. Y. Sun, X. H. Zhao, W. R. K. Illeperuma, O. Chaudhuri, K. H. Oh, D. J. Mooney, J. J. Vlassak and Z. G. Suo, *Nature*, 2012, **489**, 133–136.
41 M. Marini, B. Pourabbas, F. Pilati and P. Fabbri, *Colloids Surf., A*, 2008, **317**, 473–481.
42 L. H. Wang and J. Sheng, *J. Macromol. Sci., Part A: Pure Appl. Chem.*, 2003, **40**, 1135–1146.
43 Z. Olejniczak, M. Łęczka, K. Cholewa-Kowalska, K. Wojtach, M. Rokita and W. Mozgawa, *J. Mol. Struct.*, 2005, **744**, 465–471.
44 Z. Wu, I.-S. Ahn, C.-H. Lee, J.-H. Kim, Y. G. Shul and K. Lee, *Colloids Surf., A*, 2004, **240**, 157–164.
45 A. Kuznetsova, E. A. Wovchko and J. T. Yates, *Langmuir*, 1997, **13**, 5322–5328.
46 Y. Zhao, T. Nakajima, J. J. Yang, T. Kurokawa, J. Liu, J. Lu, S. Mizumoto, K. Sugahara, N. Kitamura and K. Yasuda, *Adv. Mater.*, 2013, DOI: 10.1002/adma.201303387.
47 J. Hu, K. Hiwatashi, T. Kurokawa, S. M. Liang, Z. L. Wu and J. P. Gong, *Macromolecules*, 2011, **44**, 7775–7781.
48 S. Rose, A. Dizeux, T. Narita, D. Hourdet and A. Marcellan, *Macromolecules*, 2013, **46**, 4095–4104.
49 H. R. Brown, *Macromolecules*, 2007, **40**, 3815–3818.
50 Y. H. Na, T. Kurokawa, Y. Katsuyama, H. Tsukeshiba, J. P. Gong, Y. Osada, S. Okabe, T. Karino and M. Shibayama, *Macromolecules*, 2004, **37**, 5370–5374.
51 J. Yang, C. Gong, F.-K. Shi and X.-M. Xie, *J. Phys. Chem. B*, 2012, **116**, 12038–12047.
52 J. Yang, L.-H. Deng, C.-R. Han, J.-F. Duan, M.-G. Ma, X.-M. Zhang, F. Xu and R.-C. Sun, *Soft Matter*, 2013, **9**, 1220–1230.
53 K. Haraguchi, K. Uyama and H. Tanimoto, *Macromol. Rapid Commun.*, 2011, **32**, 1253–1258.
54 T. Nishida, H. Endo, N. Osaka, H.-j. Li, K. Haraguchi and M. Shibayama, *Phys. Rev. E*, 2009, **80**, 030801(R).